Time resolved emission spectra and electron paramagnetic resonance studies of Gd³⁺ doped calcium phosphate glasses

Sooraj H. Nandyala[1,2*], Graham Hungerford[3], S. Babu[4], J. L. Rao[4], Isabel B. Leonor[1,2], Ricardo Pires[1,2], Rui L. Reis[1,2]

[1]*ICVS/3B's, PT Government Associated Laboratory, Braga/Guimarães, Portugal*

[2]*3B's Research Group – Biomaterials, Biodegradables and Biomimetics, University of Minho, Headquarters of the European Institute of Excellence on Tissue Engineering and Regenerative Medicine, Avepark, Barco, 4805-017, Guimarães, Portugal*

[3]*HORIBA Jobin Yvon IBH Ltd., 133 Finnieston Street, Glasgow G3 8HB, United Kingdom*

[4]*Department of Physics, Sri Venkateswara University, Tirupati 517 502, Andhra Pradesh, India*

*Corresponding author. Tel: (+351) 933420872; E-mail: nandyala.sooraj@gmail.com

ABSTRACT

Gadolinium, Gd^{3+} ($4f^7$), containing glasses are particularly interesting owing to their magnetic and optical properties. Gd^{3+} has an electron paramagnetic resonance (EPR) centre, which is often used as the EPR probe in different matrices. Another important feature of Gd^{3+} is that emits ultraviolet radiation (UVR) at around 310 – 313 nm from the $^6P_{7/2} \rightarrow ^8S_{7/2}$ transition and is suitable for the treatment of skin disease. Here, we report on Gd^{3+} doped calcium phosphate host glasses with four different concentrations; 0.5 - 4 mol % and labelled as 0.5Gd, 1Gd, 2Gd and 4Gd. A strong emission peak at 310 nm was observed in the reported glasses with excitation at 274 nm. The emission spectra can also be obtained at specific times during the decay. The time resolved emission data was analyzed with three different approaches namely, simple exponential, NED distribution and stretched exponential. The other approaches confirm the single exponential behaviour for all samples with deviation for the 0.5 Gd. The decay associated spectra (DAS) for the 0.5 Gd indicate that both decays have the same origin. The EPR spectrum exhibits several resonance signals characteristic of Gd^{3+} ions. The stimulated emission cross sections ($\sigma^P_E \times 10^{-21}$ cm²) of the UV emission transition $^6P_{7/2} \rightarrow ^8S_{7/2}$ were also reported in the above three approaches. Copyright © 2016 VBRI Press.

Keywords: Gd^{3+} glass; EPR studies; time resolved emission spectra; calcium phosphate material.

Introduction

The use of lanthanides (Ln^{3+}) doped host glasses have been a major importance in biomedical and laser applications [**1 - 4**]. Lanthanide ions have been used in medicine as anticancer drugs and radiotherapy diagnostic. For example, lanthanum carbonates, Fosrenol, as a phosphate binder for the treatment of hyperphosphatemia in renal dialysis patients in both the USA and Europe [**2**]. Further, lanthanide-doped nanoparticles that show an emerging applications in diverse areas, such as biology detection and therapy [**5**]. Various types of bioactive glasses and ceramics based on calcium phosphates host materials have been used for bone applications [**6**]. Recently, the authors have studied the development and characterization of Ce^{3+} and Sm^{3+} doped calcium phosphate glass reinforced hydroxyapatite composites for bone tissue and antibacterial applications [**7, 8**]. Among the Ln^{3+}-doped glasses, Gadolinium-containing glasses are particularly interesting owing to their magnetic and optical properties. Gadolinium most frequently occurs in the Gd^{3+} state with the ground state $^8S_{7/2}$, owing to the absence of orbital moment this ion is particularly well adapted to magnetic resonance experiments [**9**]. The importance of Gd^{3+} is that it emits ultraviolet radiation (UVR) at around 310-313 nm from the $^6P_{7/2} \rightarrow ^8S_{7/2}$ transition and is suitable for the treatment of skin diseases, like psoriasis, vitiligo, atopic dermatitis (eczema) and other photo responsive skin disorders[**10**]. UVR can be generally divided into three categories, UVA - ultraviolet A at wavelength 400–320 nm, UVB - ultraviolet B at 320–280 nm, and UVC - ultraviolet C at 280–200 nm. More than 98 % of UVA radiation reaches the surface of the earth and UVB radiation is absorbed by the atmosphere; with only <2 % of UVB radiation reaching the earth surface. UVC radiation is completely scattered and absorbed by O_3, O_2, and N_2 in the atmosphere [**11**]. In recent years, UVB has been extensively used in a variety of applications such as production of vitamin D, transcription of repair enzymes, etc [**12, 13**].

Time-resolved emission spectroscopy (TRES) may be extremely effective in samples that present a huge amount of emitting centres simultaneously. With the steady state technique only the most intense emitting or longer-lived centres are preferentially detected, while the weaker ones

can remain unnoticed. Therefore, using the time-resolved emission it is possible to obtain more quantifiable data. In TRES, the emission spectra can be obtained at specific times during the decay. Further, TRES can also be used to assist structural studies. This technique is very sensitive to the kind of active ion, its local site and distribution within the host matrix. It is possible to identify overlapped bands, if they have origin in processes with different lifetimes. Earlier, the authors reported TRES spectra for Er and Nd doped different host glasses [14, 15]. TRES analysis reveals that, because of network randomness, the luminescence emissions do not present the same lifetime or wavelength for the same bands. This can be attributed to different environments (or interactions) experienced by erbium ions, which are responsible for emissions with different decay times and energy [14]. Time-resolved luminescence measurements can provide interesting information on the local environment of the luminescent species, on the isotropy of the glass type and on energy transfer processes [16]. The strong change of the lifetime behaviour with increasing lanthanide doping can relate to an inhomogeneous distribution. This leads to clustering of the Ln^{3+} ions in different local sites but without phase separation of the glass network [17].

Furthermore, lanthanides can be considered as a probe and used to determine the environmental symmetry of the complexes in their host lattices. Therefore, electron paramagnetic resonance (EPR) spectroscopy has emerged as an efficient tool for the characterization of local order in a variety of solid-state systems. In fact, Gd^{3+} has an EPR centre, which is often used as the EPR probe in different matrices. The authors have employed EPR studies for different host glassy and phosphor materials [18, 19]. For example, the electron paramagnetic resonance studies were carried out on $LiGa_5O_8$:Mn^{2+} powder phosphor at room temperature and at 110 K. The resultant EPR spectrum exhibits resonance signals characteristic of Mn^{2+} ions. It is observed that the spin-Hamiltonian parameters (g) and splitting constant (A) do not vary with temperature [18]. In another report, the EPR studies in mixed alkali borophosphate glasses doped with a small amount of paramagnetic impurity MnO was carried out. The EPR spectra of Mn^{2+} ions in the glasses exhibit a resonance signal with effective g value at $g = 2.02$ with six line hyperfine structure (hfs). The resolved hfs indicates that the paramagnetic ion is in the divalent state and the site symmetry is distorted octahedral [19]. Therefore, the present letter brings out an analysis on the ultra violet radiation transition $^6P_{7/2} \rightarrow {}^8S_{7/2}$ of Gd^{3+} doped 0.5-4 mol % in terms of time resolved data and EPR measurements.

Experimental

Preparation of Gd³⁺ doped calcium phosphate host glasses

Gd_2O_3 doped calcium phosphate glasses have been prepared by the quenching technique. Briefly, they were obtained by melting the mixture of analytical grade CaF_2, Na_2CO_3, CaO , P_2O_5, and Gd_2O_3 raw chemicals (Sigma Aldrich, 99.99% purity), in crucibles, for about an hour in

an electrical furnace at temperature of 1000-1100 °C, with the following chemical composition:

- 0.5 Gd: $10CaF_2$-$10Na_2CO_3$-$15CaO$-$64.5P_2O_5$- 0.5 Gd_2O_3
- 1 Gd: $10CaF_2$-$10Na_2CO_3$-$15CaO$-$64P_2O_5$ - 1 Gd_2O_3
- 2 Gd: $10CaF_2$-$10Na_2CO_3$-$15CaO$-63 P_2O_5 - 2 Gd_2O_3
- 4 Gd: $10CaF_2$-$10Na_2CO_3$-$15CaO$-$61P_2O_5$ - 4 Gd_2O_3

The resultant glasses were circular in design, with 2–3 cm in diameter, with a thickness of 0.33 - 0.38 cm, and have good transparency. The glasses were then annealed at 200 °C for an hour, to remove thermal strains.

Characterization techniques for Gd³⁺ doped calcium phosphate host glasses

Glass density was measured using water as an immersion liquid by Archimedes' principle on a Mettler Toledo balance. An Abbe refractometer was used to measure the glass refractive index.

Time-resolved measurements of Gd^{3+} doped calcium phosphate host glasses: Measurements were performed on a HORIBA Scientific Delta Flex equipped with a Spectra LED excitation source, emitting at 274 nm, and a PPD-850 detector. Time-resolved emission spectra (TRES) were made by recording the time-resolved decay at equal wavelength steps for a fixed time period. This produced an intensity – wavelength – time, i.e. 3-D, dataset. Both simple decay and global analysis of the TRES data was performed using DAS6 software. Decays were fitted as a sum of exponential components of the form;

$$I(t) = \sum_{i}^{n} \alpha_i \exp(-t / \tau_i) \tag{1}$$

With the "amount" of each luminescent component represented by the normalised pre-exponential factor, i.e;

$$\alpha_i = \frac{\alpha_i}{\sum_{i=1}^{n} \alpha_i} \tag{2}$$

Single decay data were also treated using a lifetime distribution model (NED module in DAS6) as we have previously used with lanthanide-glass systems [14] and proteins [20]. Monitoring the "q" parameter is also indicative if distribution or exponential in nature (i.e. q =1 indicates exponential in nature, q > 1.01 distribution). A stretched exponential model based on the Kohlrausch function, see below was also employed.

$$F(t) = A + B_1 \exp\left[-\left(\frac{t}{T_1}\right)^{\beta}\right] \tag{3}$$

where, T_1 is the lifetime and β is the stretch factor with the following range $0 < \beta \leq 1$. At β = 1 the function behaves as an ordinary exponential function. Goodness of fit was assessed by evaluation of the reduced chi-squared value and weighted residuals. The outcomes of the global analysis of the TRES data were then treated to produce decay associated spectra by plotting (using Origin software) the pre-exponential components (see eq. 2), weighed by their lifetime, against wavelength.

Electron paramagnetic resonance (EPR) studies of Gd^{3+} doped calcium phosphate host glasses: A powdered glass sample of 100 mg was taken in a quartz tube for the EPR measurements. The EPR spectra of the sample were recorded on a JEOL FEIX ESR spectrometer operating in the X-band frequencies, with a field modulation of 100 kHz.

Table 1. Physical properties of Gd^{3+} (0.5-4 mol %) doped calcium phosphate host glasses.

Physical properties	Symbol/units	Gd₂O₃ doped calcium phosphate glasses				Formula/Method
		0.5	1	2	4	
1. Density	ρ (g/cm³)	2.525	2.550	2.630	2.722	Archimedes principle
2. Refractive Index	n_d	1.499	1.500	1.503	1.509	Abbe Refractometer
3. Lanthanide ion concentration	$N_{Gd}(10^{22}$ ionscm⁻³)	0.633	1.267	2.566	5.129	$\left[N_A \times \dfrac{M\% RE}{\overline{M}} \times d\right]$
4. Polaron radius	$r_p\left(\overset{\circ}{A}\right)$	2.178	1.729	1.366	1.085	$\dfrac{1}{2}\left[\dfrac{\pi}{6N}\right]^{1/3}$
5. Interionic distance	$r_i\left(\overset{\circ}{A}\right)$	5.408	4.290	3.390	2.691	$\left[\dfrac{1}{N}\right]^{1/3}$
6. Field strength	F(10¹⁶cm²)	0.211	0.335	0.536	0.849	$\left[z/r_p^2\right]$

where, $\overline{M}$ = Average molecular weight; N_A= Avogadro's Number; M % RE=Mole percent of Lanthanide ion (Gd^{3+}); N = Lanthanide ion concentration; Z= Oxidation number

Results and discussion

Physical properties of Gd^{3+} doped calcium phosphate host glasses

Table1, presents the physical properties, such as density (d) refractive index (n_d), Gd^{3+} ion concentration (N_{Gd}^{3+}), polaron radius (r_p), inter ionic distance (r_i) and field strength (F) of Gd^{3+} (0.5-4mol %) doped calcium phosphate glasses. The density and average molecular weight values have been used in evaluating the number of luminescent ions (N_{Gd}^{3+}). The ion-ion interactions in these glasses are very densely distributed. The polaron radius (r_p) is 2.5 times smaller in comparison with the inter-ionic distance (r_i) and hence these smaller (r_p) values have resulted in a higher field strength (F). As glass network is crowded by Gd^{3+} interstices, Gd-O bond strength increases. The increasing Gd-O bond strength produces stronger field strength (F) around Gd^{3+} ions and therefore compactness of glass structure has increases with the addition of Gd_2O_3 [21].

Electron paramagnetic resonance (EPR) studies of Gd^{3+} doped calcium phosphate host glasses

EPR spectral studies were carried out at room temperature for all the concentrations of Gd^{3+} ion and are shown in **Fig. 1**(**A** & **B**), as specimen for 1Gd and 4Gd. The EPR spectrum for 1 mol % Gd shows several resonance signals with an effective g values g ≈ 1.97, 2.72, 3.39, 4.38 and 5.80. At higher concentration of Gd^{3+} ion (4 mol %), an intense resonance signal at g ≈ 2.06 is observed. In addition to this another resonance signal is observed at g ≈ 6.42. Gd^{3+} has a 4f⁷ configuration, the ground state being ⁸S₇/₂ with L= O. The characteristics of Gd^{3+} ions are different when compared with the other rare earth ions because of zero angular momentum.

It is well established in many Gd^{3+} studies [22] that spectral characteristics strongly depend on the relative magnitude of Zeeman microwave frequency and ligand field strength. In the particular case of a very weak crystal field, a single resonance line at g ≈ 2.0 will be observed. As L= O, a crystal field alone cannot split an S state. The splitting originates from higher order perturbations involving spin-orbit coupling and spin-spin coupling. The strong spin-orbit coupling of 4f electrons breaks the L-S scheme of energy levels and the ground multiplet is mixed with L0 states which result in large crystal field interactions. In such a case, the EPR spectrum of Gd^{3+} ions is characterized by several lines, which depend on the local symmetry of Gd^{3+} ion and the magnitude of crystal field (CF) interaction. The expected EPR spectrum for different magnitudes of crystal field interaction (HCF) in relation to the Zeeman splitting is measured by hv (where v is the microwave frequency) and has been described in detail elsewhere [**22**]. In the weak crystal field region, HCF/hv ≤ ¼, higher order transitions are forbidden and the spectra are observed in the g ≈ 2.0 region. Intermediate CF region has been considered in two parts (a) lower intermediate and (b) higher intermediate CF regions. In the lower intermediate region (1/4 ≤ HCF/hv ≤ 1), EPR spectrum will be observed over a wide region wherever g varies over the values 2.0 < g < ∞. For the case of higher intermediate CF region, a group of resonance signals with g ≥ 2.0 is expected. In the strong CF case, EPR spectrum will be determined by transitions within the Kramers doublets. In the present work, several resonance signals are observed in the low field region for 1 mol %. Gd^{3+} ion. The spectrum resembles with the typical U spectrum with effective g values at g ≈ 5.6 - 6.0, 2.8 - 2.8, 1.9 -2.0 [23]. The U spectrum changes into a broad peak with g ≈ 2.06 as the concentration of Gd^{3+} ion increases (4 mol %). The resonance signal at g ≈ 6.42 is attributed to Gd^{3+} ion with intermediate CF strength [**24**].
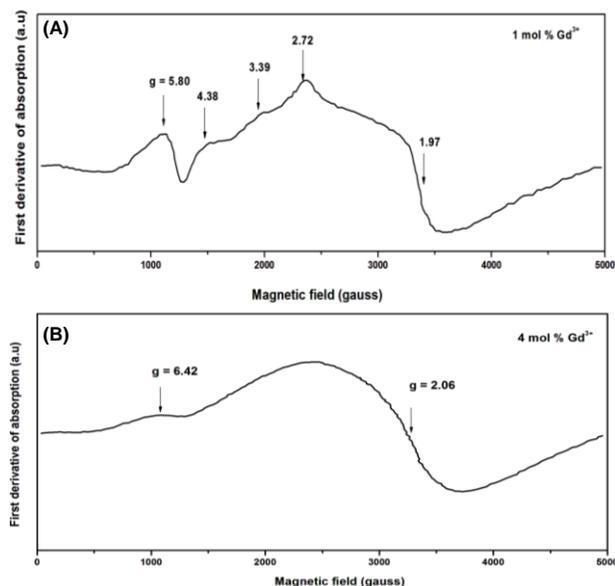
Fig. 1. EPR spectrum of Gd^{3+} doped (A) 1 mol % ;(B) 4 mol% calcium phosphate host glasses.

UV luminescence and time resolved emission spectral studies of Gd^{3+} doped calcium phosphate host glasses

Recently, Gadolinium ions have appeared attractive sources of ultraviolet (UV) light emission for biomedical

applications in the UV type B light (280-320 nm) region. In order to examine the concentration effect, the UV luminescence spectra of 0.5-4 mol % doped calcium phosphate glasses have been recorded with an excitation at 274 nm, as shown in **Fig. 2A**. The observed emission transitions showed two bands; one at 310 nm ($^6P_{7/2} \rightarrow {}^8S_{7/2}$) and another band $^6P_{5/2} \rightarrow {}^8S_{7/2}$ at 304 nm. The main transition ($^6P_{7/2} \rightarrow {}^8S_{7/2}$) is very sharp peak in the higher concentration of 1Gd, 2 Gd and 4 Gd calcium phosphate glasses. This peak is somehow different for the 0.5 Gd sample, due to the fact that lanthanide ion concentration (N_{Gd} 10^{22} ions cm^{-3}) is very low, 0.633, compared to the others. Furthermore, the second transition $^6P_{5/2} \rightarrow {}^8S_{7/2}$ at 304 nm was only observed in the higher concentration (2Gd and 4 Gd) samples because of the formation of Gd ion clusters in the glass matrix at these concentrations. The **Fig. 2B** shows the decay curves (sum decays) of the Gd glasses with excitation at 269 nm. In a simple exponential way (i), the luminescence intensity $I(t)$ is well modelled by the sum of two exponential decay components i.e., $I(t)=A_1 \exp(-t/\tau_1)+A_2 \exp(-t/\tau_2)$ where τ_1 and τ_2 are the short and long lifetimes with corresponding intensity coefficients A_1 and A_2, respectively as simple exponential decay analysis.
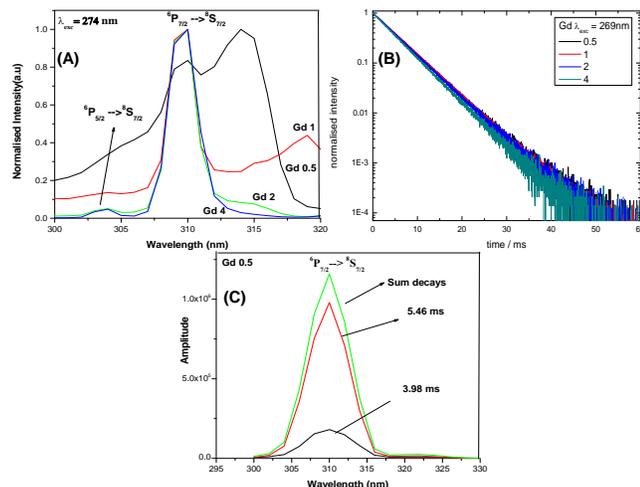
Fig. 2. (A) UV luminescence spectra of 05-4 mol% of Gd; (B) Decay curves (life times) (i.e. sum decays) of 0.5-4 mol% Gd doped calcium phosphate host glasses, and (C) Decay associated emission (DAS) spectra of Gd^{3+} doped (0.5mol %) calcium phosphate host glass.

Table 2. Lifetimes of the 0.5-4 mol % Gd doped calcium phosphate host glasses with three different approaches.

Samples	(i) Simple exponential				(ii) NED Distribution		(iii) Stretched exponential	
Gd	τ_1	τ_2	α_1	α_2	τ	q	τ	β
0.5	5.46		3.980.780.22		5.08	1.011	5.06	0.98
1	5.29		1		5.29	1.000	5.29	1.00
2	5.13		1		5.12	1.001	5.11	1.00
4	4.85		1		4.83	1.002	4.83	1.00

The data have also been analyzed in several other ways by (ii) NED–distribution analysis and (iii) Stretched exponential. The other approaches (ii) and (iii) really confirm the exponential nature of the decay for all samples, with a slight deviation for the 0.5 Gd glass. **Table 2** show

the decay curves (life times) data for the 0.5 - 4 Gd glasses with three different approaches.

On the analysis of the time-resolved emission spectra (TRES) data, i.e. to obtain the decay associated spectra (DAS), it is possible to visualize the emission spectra related to the different decay times as shown in **Fig. 2C** of 0.5 Gd sample. This is not possible using the steady state approach. Considering the 5.46 ms decay time, the UV emission sharp and prominent band at 310 nm ($^6P_{7/2} \rightarrow {}^8S_{7/2}$) was clearly monitored. The latter band is also prominent in the spectra associated with the other decay time (3.98 ms), which may be indicative of heterogeneous host microenvironments. Moreover, the sum decay was also seen in the **Fig. 2C**. The decay associated spectra (DAS) for the 0.5Gd seem to indicate that origin of both decays the same (as have same spectrum). Therefore, only the 0.5 Gd seems to deviate from single exponential behaviour and the DAS are presented for this sample.

The evaluation of the stimulated-emission cross-section (σ^E_P) is considered to be an important factor to understand the emission performance of an optical glass. Therefore, from the emission spectral profile of the glass, the emission peak wavelengths (λ_p nm), effective band width at half maximum (FWHM) ($\Delta_{\lambda p}$ nm) and stimulated emission cross-sections of the measured emission levels were calculated from equation given below:

$$\sigma^E_P = (\lambda_p^4 / 8\pi c n_d^2 \Delta_{\lambda p}) \times A (= \tau_m^{-1}) \qquad (4)$$

where, λ_p is the wavelength of emission peak and $\Delta_{\lambda p}$ is the effective half width of the emission bands (FWHM), C is the velocity of the light, n_d is the refractive index of the glass and A is the transition probability or the emission peak's inverse lifetime (τ_m^{-1}) value. From the luminescence spectra of all the Gd glasses, the emission level wavelength (λ_P nm), effective bandwidth ($\Delta\lambda_P$ nm) and stimulated emission cross-section ($\sigma_P^E \times 10^{-21}$ cm^2) of the Gd^{3+} doped calcium phosphate glasses were evaluated for the UV luminescence transition ($^6P_{7/2} \rightarrow {}^8S_{7/2}$) and tabulated in **Table 3**.

Table 3. Emission, FWHM, stimulated emission cross-sections and lifetimes of the UV emission Gd^{3+} (0.5-4.0%) doped calcium phosphate glasses.

Gd	Excitation Transitions	λ_{exe} /nm	Emission Transition	λ_{em} /nm	FWHM ($\Delta\lambda_p$ nm)	Stimulated emission cross- sections (σ^P_e X10^{-21}cm^2)	$\tau_{mea(ave)}$ /ms
				(i) Simple exponential			
0.5	$^8S_{5/2} \rightarrow {}^6I_J$	274	$^6P_{7/2} \rightarrow {}^8S_{7/2}$	314	9	0.117	5.46
1	$^8S_{5/2} \rightarrow {}^6I_J$	274	$^6P_{7/2} \rightarrow {}^8S_{7/2}$	310	2	0.515	5.29
2	$^8S_{5/2} \rightarrow {}^6I_J$	274	$^6P_{7/2} \rightarrow {}^8S_{7/2}$	310	2	0.528	5.13
4	$^8S_{5/2} \rightarrow {}^6I_J$	274	$^6P_{7/2} \rightarrow {}^8S_{7/2}$	310	2	0.555	4.85
				(ii) NED –Distribution analysis			
0.5	$^8S_{5/2} \rightarrow {}^6I_J$	274	$^6P_{7/2} \rightarrow {}^8S_{7/2}$	314	9	0.125	5.08
1	$^8S_{5/2} \rightarrow {}^6I_J$	274	$^6P_{7/2} \rightarrow {}^8S_{7/2}$	310	2	0.514	5.29
2	$^8S_{5/2} \rightarrow {}^6I_J$	274	$^6P_{7/2} \rightarrow {}^8S_{7/2}$	310	2	0.529	5.12
4	$^8S_{5/2} \rightarrow {}^6I_J$	274	$^6P_{7/2} \rightarrow {}^8S_{7/2}$	310	2	0.557	4.83
				(iii) Stretched analysis			
0.5	$^8S_{5/2} \rightarrow {}^6I_J$	274	$^6P_{7/2} \rightarrow {}^8S_{7/2}$	314	9	0.126	5.06
1	$^8S_{5/2} \rightarrow {}^6I_J$	274	$^6P_{7/2} \rightarrow {}^8S_{7/2}$	310	2	0.515	5.29
2	$^8S_{5/2} \rightarrow {}^6I_J$	274	$^6P_{7/2} \rightarrow {}^8S_{7/2}$	310	2	0.531	5.11
4	$^8S_{5/2} \rightarrow {}^6I_J$	274	$^6P_{7/2} \rightarrow {}^8S_{7/2}$	310	2	0.557	4.83

Therefore, the stimulated emission cross-section of the measured UV emission band exhibits a similar emission performance among all the glasses and except 0.5 Gd in three different approaches as shown in table. Further, the

0.5 Gd calcium phosphate glass emission performances were deviated due to the concentration effect in the glass matrix.

Conclusion

In this letter new calcium phosphate host glasses have been developed with four different concentrations of Gadolinium oxide. The time-resolved emission spectra and Electron Paramagnetic Resonance studies were reported. The EPR spectrum of Gd^{3+} doped Calcium phosphate glasses (1 mol %) exhibits resonance signals with effective g values at g ≈ 1.97, 2.72, 3.39, 4.38 and 5.80. For higher concentrations of Gd^{3+} ions two resonance signals are observed at g ≈ 2.06 and g ≈ 6.42. The signals with effective g values at g ≈ 1.97, 2.06 and 2.72 are attributed to Gd^{3+} ions in weak cubic symmetry field. The resonance signals with the effective g values at g ≈ 3.39, 4.38, 5.80 and 6.42 are attributed to Gd^{3+} ions in an intermediate and strong cubic symmetry field. Further, the time resolved emission data have been analyzed with three different approaches namely, simple exponential, NED distribution and stretched exponential, and confirms the exponential nature of the decay for all the samples. In fact, Ultraviolet (UVB) radiation has been extensively used in a variety of applications such as production of vitamin D and in the treatment of skin diseases. Therefore, the need of UV emitting materials giving light output in well-defined spectral region is very important for phototherapy lamps applications. Eventually, the reported glasses (1Gd, 2Gd and 4Gd) show an efficient UVB light transition at 310 nm, and the calcium phosphate host glass is a good candidate for UVB laser performance.

Author Contributions

All authors contributed equally to the work. Authors have no competing financial interests.

Reference

1. Kui, W.; Li. R.; et al.; Coord. *Chem. Rev.,* **1999**, *297*, 190.
   DOI: 10.1016/S0010-8545(99)00072-7
2. Fricker, S.P; *Chem. Soc. Rev.*, **2006**, *35*, 524.
   DOI: 10.1039/b509608c
3. Barta, C. A.; Sachs-Barrable, K.; et al.; *Dalton Trans.,* **2007,** *43*, 5019.
   DOI: 10.1039/b705123a
4. Sooraj Hussain, N.; Santos, J.D. (Eds.); Trans Tech Publisher: Switzerland, **2008.**
5. Hongli, W.; Feng, W.; Lanthanide-Doped Nanoparticles: Synthesis, Property, and Application, In Nanocrystalline Materials (Second Edition), Sie-Chin Tjong (Eds.), Elesiver, London, **2014**, pp.121-160.
   DOI: 10.1016/B978-0-12-407796-6.00004-X
6. Sooraj Hussain, N.; Santos, J.D. (Eds.); Trans Tech Publisher: Switzerland, **2010.**
7. Morais, D.S.; Fernandes, S.; et al.; *Biomed. Mater*., **2015**, *10*, 055008.
   DOI: 10.1088/1748-6041/10/5/055008
8. Morais, D.S.; Coelho, J.; et.al; *J. Mater. Chem. B*, **2014**, *2*, 5872.
   DOI: 10.1039/C4TB00484A
9. Srinivasulu, K.; Omkaram, I.; et al; *J. Mol. Struct.* **2013**, *63*, 1036.
   DOI: 10.1016/j.molstruc.2012.09.041
10. Mokoena, P. P.; Nagpure, I. M.; Kumar, V et al.; *J. Phys Chem Solids,* **2014**, *75*, 998.
    DOI: 10.1016/j.jpcs.2014.04.015
11. Chien-Hao, H.; Teng-Ming, Chen.; Bing-Ming, C; *Inorg. Chem.*, **2011**, *50*, 6552.
    DOI: 10.1021/ic2001877
12. Singh, V.; Sivaramaiha, G.; Rao, J.L.; Kim, S. H; *J. Electron. Mater.,* **2014**, *43*, 3486.
    DOI: 10.1007/s11664-014-3091-8
13. José A. J.; *Mater. Lett.,* 2015, 159, 193.
    DOI: 10.1016/j.matlet.2015.06.110
14. Coelho, J.; Hungerford, G.; Sooraj Hussain, N; *Chem. Phys. Lett.,* **2011**, *512,* 70.
    DOI: 10.1016/j.cplett.2011.07.019
15. Coelho, J.; Hungerford, G.; Sooraj Hussain, N; *Solid State Phenomena,* **2014**, *207*, 37.
16. Herrmann, A.; Fibikar, S.; Ehrt, D; *J. Non-Cryst. Solids*, **2009**, *355*, 2093.
    DOI: 10.1016/j.jnoncrysol.2009.06.033
17. Andreas, H.; Ehrt, D; *J. Non-Cryst Solids*, **2008**, *354*, 916.
    DOI:10.1016/j.jnoncrysol.2007.08.040
18. Vijay, S.; Chakradhar, R.P.S.; Rao, J.L.; Dong-Kuk, K; *J. Lumin*., **2009,** *129*, 755.
    DOI:10.1016/j.jlumin.2009.02.009
19. Kesavulu, C.R.; Muralidhara, R.S.; Rao J.L.; Anavekar, R.V.; Chakradhar, R.P.S; *J. Alloys Compd*., **2009**, *486,* 46.
    DOI:10.1016/j.jallcom.2009.07.040
20. Sagoo, K.; Hirsch, R.; et al.; *Spectrochim. Acta A*., **2014**, *124,* 611.
    DOI: 10.1016/j.saa.2014.01.073
21. Ramteke, D.D., Gedam, R. S; *J. Rare Earths*, **2014**, *32*, 389.
    DOI: 10.1016/S1002-0721(14)60082-X
22. Brodbeck, C.M.; Iton, L.E; *J. Chem. Phys.*, **1985**, *83*, 4285.
    DOI: 10.1063/1.449041
23. Rao, K. K..;Anantharamulu, N.; Salagram, M.; Vithal, M; *Spectrochim.Acta A.,* **2007**, *66*, 646.
    DOI: 10.1016/j.saa.2006.04.005
24. Koopmans H.J.A, Eprik, M.M, Nieuwentuijise, B., Gellings, P. J; *Phys. Status Solidi* b, **1983**, *120,* 745.
    DOI: 10.1002/pssb.2221200234

.